THE AMERICAN SOCIETY OF MECHANICAL ENGINEERS
345 E. 47th St., New York, N.Y. 10017

98-GT-342

A COMPUTATIONAL MODEL FOR THE STUDY OF GAS TURBINE COMBUSTOR DYNAMICS

David M. Costura, Patrick B. Lawless, Steven H. Frankel

Thermal Science and Propulsion Center
School of Mechanical Engineering, Purdue University
West Lafayette, IN 47907

ABSTRACT

A dynamic combustor model is developed for inclusion into a one-dimensional full gas turbine engine simulation code. A flux-difference splitting algorithm is used to numerically integrate the quasi-one-dimensional Euler equations, supplemented with species mass conservation equations. The combustion model involves a single-step, global finite-rate chemistry scheme with a temperature-dependent activation energy. Source terms are used to account for mass bleed and mass injection, with additional capabilities to handle momentum and energy sources and sinks. Numerical results for cold and reacting flow for a can-type gas turbine combustor are presented. Comparisons with experimental data from this combustor are also made.

INTRODUCTION

Due to the inherent dynamics of the fluid system, the transient performance of a gas turbine engine can differ significantly from that predicted from quasi-steady operating assumptions. The consequences of these dynamics can be quite dramatic, including unexpected crossing of the compressor surge line while transitioning between operating points. Beyond the surge line, compressor rotating stall and surge serve as the forcing functions for a complex dynamic interaction between the engine components. These unsteady operating cycles are of particular interest, as they result in substantially reduced performance and durability. Recovery from rotating stall and surge is an important issue facing the gas turbine designer, since it is impossible to guarantee that an engine can avoid such behavior during its operational lifetime. Because of this, significant efforts have been made to accurately simulate the performance of a compressor undergoing a surge transient (Hale and Davis, 1992). As these techniques have matured, the focus increasingly has shifted toward extending these methods to encompass the entire engine, and thus capture the important compressor-combustor interactions that occur during engine surge (Garrard et al., 1995; Garrard, 1995). One of the more challenging tasks in this effort is the modeling of combustor behavior.

In the earliest days of gas turbine engine development, combustor design was regarded as somewhat of a 'black art,' typically involving labor intensive parametric testing. As the 'art' evolved into more of a science, rule-based design techniques relying on experimental correlations became an important part of the initial design phase (Lefebvre, 1983). More recently, as industry was challenged by ever more stringent requirements for performance and emissions, advanced computational modeling has played an important role in the design sequence. Ideally, a combustor model would address the actual physical processes, including the effects of three-dimensional, turbulent, viscous, reacting flow. Unfortunately, such models require vast computational resources that prohibit their use as a design tool. As a result, numerous efforts have been made over the past 35 years to produce simplified models to predict gas turbine combustor performance (Lefebvre, 1983). These models and numerical techniques have primarily focused on the simulation of steady flow in combustors, with particular emphasis in the past 20 years on pollution (Mellor, 1976; Gupta and Lilley, 1994). Considering the modeling difficulties experienced in steady flow, it is not surprising that little effort has been directed on addressing the added complexity of the transient behavior of the combustor. Unfortunately, the limited knowledge in this area has proven a key difficulty in modeling dynamic gas turbine engine behavior, especially post-stall dynamics.

Pryzbylko (1985) identified the important role the combustor played in determining an engines ability to recover from surge. He also presented one of the first discussions concerning modeling efforts in post-stall engine dynamics which addressed the desired features of a post-stall dynamic combustor model. Coincident with Pryzbylko's discussion of transient engine modeling, Davis (1986) modified a one dimensional time dependent stage-by-stage axial compressor model to describe the behavior of a high-speed compression system during post-stall events. This model was finite-volume based, and solved the one-dimensional Euler equations. It incorporated a time-lagged source term treatment to provide a dynamic stage characteristic in the rotating stall region. This treatment alleviated the problems associated with applying the quasi-steady assumption to events such as rotating stall and surge which were primary concerns of Pryzbylko.

To capture the effect of the combustor on system stability, further refinements of this model introduced a set of control volumes representing the combustor geometry. Heat released from the reaction was evenly distributed throughout the entire combustor section, with the presence of a flame based upon fixed equivalence ratio criterion. Similar to the approach taken for the compressor model, an ignition delay was imposed which lagged the heat release

Presented at the International Gas Turbine & Aeroengine Congress & Exhibition
Stockholm, Sweden — June 2–June 5, 1998
This paper has been accepted for publication in the Transactions of the ASME
Discussion of it will be accepted at ASME Headquarters until September 30, 1998

during re-light with a time constant taken from experimental measurements, analogous to the treatment of the turbomachinery terms that were included.

Over the last decade, the work of Davis evolved into the Aerodynamic Turbine Engine Code (ATEC) whose latest results are presented by Garrard (1995). This type of model has demonstrated its effectiveness in characterizing the dynamics of the gas turbine, albeit with certain limitations. One of these limitations is the accuracy with which the model can characterize the combustor behavior. The simple quasi-steady heat release formulation employed in the model has limited ability to accurately predict heat release, flame-out, re-light, and fuel migration in the combustor. Despite these limitations, the current models have shed new light on the importance of the compressor-combustor interaction during the engine surge event.

To improve the accuracy of such engine simulations, it is evident that an improved combustor model is necessary. A key to producing this improved model is the ability to model fuel transport, as this is critical to the calculation of the local equivalence ratio. As this local equivalence ratio is the basis for all of the empirical combustor dynamic calculations of the ATEC model, in itself including fuel transport would be a significant improvement. However, a significant additional benefit of adding fuel transport modeling is the ability to incorporate finite rate chemical kinetics which allows for the prediction of both the magnitude and location of the heat release due to combustion, thus removing significant empiricism from the analysis.

The objective of the research discussed herein is to develop a computational combustor model based on finite-rate chemistry for incorporation into a dynamic gas turbine engine model. The goal of the model under development focuses on characterizing the type of dynamic events typical of aircraft engine operation. Initial verification of this model was accomplished by comparison to step-combustor studies (Costura et al., 1997). As favorable agreement was achieved, computational studies herein are now focused on realistic gas turbine combustor geometry. Specifically, the model that is developed will be exercised against the geometry of a can-type gas turbine combustor currently being tested at Purdue as part of this research effort.

TECHNICAL APPROACH

As the objective of this work is to develop a dynamic combustor model for incorporation into the ATEC full gas turbine engine simulation code, the same modeling philosophy and numerical approach used in ATEC (Garrard, 1995) is employed here. The model is then evaluated on the geometry from a can type gas turbine combustor which has been tested at Purdue (Costura, 1997).

Governing Equations

The unsteady quasi-one-dimensional Euler equations, supplemented with the species mass conservation (neglecting molecular transport) are numerically integrated using a first-order, characteristic-based, explicit finite-difference method (Kneile and Hale, 1995). The governing equations, expressed in vector conservative form, are:

$$\frac{\partial \bar{U}}{\partial t} + \frac{\partial \bar{F}}{\partial x} = \bar{G} \qquad (1)$$

$$\bar{U} = \begin{bmatrix} S\rho \\ S\rho u \\ SE \\ S\rho Y_i \end{bmatrix} \qquad (2)$$

$$\bar{F} = \begin{bmatrix} S\rho u \\ S(\rho u^2 + P) \\ S(E + P)u \\ S\rho Y_i u \end{bmatrix} \qquad (3)$$

$$\bar{G} = \begin{bmatrix} \dot{m}_b + \dot{m}_{inj} \\ P\dfrac{dS}{dx} + F_{blade} + F_b - F_l - F_s \\ W_s + \dot{Q}_{chem} + \dot{H}_b + \dot{H}_{inj} + \dot{E}_{ign} \\ \dot{m}_b Y_i + \dot{m}_{inj} Y_i + \dot{\omega}_i \end{bmatrix} \qquad (4)$$

where ρ, u, E, P, Y_i, and S are the density, velocity, total energy (sensible, chemical and kinetic), pressure, i^{th} species mass fraction, and cross-sectional area, respectively. The source vector G contains mass, momentum, energy and species source/sink rate terms per unit length. In the conservation of mass equations (total and individual species), $\dot{m}_b$ represents the mass transfer rate across boundaries other than the inlet or exit (such as secondary or dilution air addition), and $\dot{m}_{inj}$ represents mass addition due to fuel injection. In the momentum equation, the first term is due to the cross-sectional area variation, while the remaining terms are due to blade forces (not used here), bleed momentum losses, flow losses, and skin friction losses, respectively. In the energy equation, the source terms represent shaft power (not used here), chemical energy release, enthalpy gain due to mass addition and thermal energy deposition due to ignition, respectively. In the species mass conservation equation, the source terms represent mass addition due to dilution air and fuel injection, and the chemical production term. Under the assumption of an ideal gas mixture and cold air-standard assumptions, the equation of state is:

$$P = (\gamma - 1)(E - \frac{\rho u^2}{2}) \qquad (5)$$

where γ is the ratio of the specific heats.

The formulation and major assumptions of the model are made to be consistent with the ATEC approach and may be extended and relaxed in future work.

Combustion Model.

Hydrocarbon fuel combustion is modeled with a single-step, global chemical reaction mechanism based upon the work of Westbrook and Dryer (1981), which is of the form:

$$C_xH_y + (x + y/4)O_2 \rightarrow xCO_2 + (y/2)H_2O \qquad (6)$$

After testing numerous mixtures of fuel and oxidizer, Westbrook and Dryer were able to develop a set of reaction rate parameters which provided excellent agreement between experimental and predicted flame speeds and flammability limits. The reaction rate equation used takes the form of the Arrhenius equation :

$$\dot{\omega}_{C_xH_y} = \frac{d\left[C_xH_y\right]}{dt} = -A\exp\left(-\frac{E_a}{RT}\right)\left[C_xH_y\right]^a\left[O_2\right]^b \qquad (7)$$

where the parameters R_u, A, E_a, a, and b, represent the universal gas constant, pre-exponential factor, activation energy, and concentration exponents respectively. The last four terms are the parameters that were adjusted to match experimental data accumulated during their studies. The study performed by these authors was primarily based upon temperatures in excess of 1000 K which are typically encountered in steady flames. In transient simulations, where ignition phenomena are important, using a constant activation energy, E_a, can lead to undesirable results. Of primary concern is the low temperature kinetics which dominate during this period of the combustion process. Generally, in order to describe an ignition event, significant modifications need to be implemented to produce a stable solution (Winowich, 1990)

Ignition is dependent upon the formation of free-radical species which develop as a result of the ignition source, usually a spark. These free-radicals are not modeled in a global one-step combustion mechanism because these species are simply intermediate products which are subsequently decomposed as the reaction reaches, ideally, completion characterized by the ultimate production of carbon dioxide and water vapor. With their absence, there is no physical mechanism for ignition delay which in term causes extremely rapid increases in chemical heat release often driving computational models to instability. Several methods have been proposed and tested to overcome this weakness in the chemical model:

- Incorporation of a minimal number of additional chemical reactions. Typically at least 5-7 chemical equations involving generally ten additional chemical species are necessary to have the desired effect (Vlachos, 1996; Egolfopoulos et al., 1992).
- A two-step chemistry mechanism which divides the overall reaction rate into disparate temperature ranges. When the local temperature is below a lower temperature threshold, a low temperature global mechanism is used to model ignition events. For high temperature combustion, typically over 1100 K, the models use another single step global mechanism. Finally, while in the region between the lower threshold and high temperature regime, a representative average of the two rates is employed (Kong and Reitz, 1993; Ayoub and Reitz, 1997).
- Modification of one or more of the reaction rate parameters while still using a single global chemical kinetics mechanism (Winowich, 1990; Segal and Haj-Harra, 1994; Chitsomboon and Notham, 1991).

In this study, the later method was chosen, as the primary motivation for using a quasi-one-dimensional model is to balance the computational workload with the requirement for a physics-based dynamic model. Thus, the inclusion of more than a half-dozen additional species conservation equations was not regarded as a worthwhile investment of computational resources in this context. And although the use of multiple global kinetics mechanisms over a few temperature regimes does not increase the computational time significantly, the approach has been used principally in multidimensional analysis of complex flows. Without any documented efforts in one dimensional flows, the data base presented in the literature was not directly applicable. Thus, upon evaluation of the probability of success, this technique was viewed with less enthusiasm than the single mechanism implementation.

The principle task in impelmenting the single global kinetics method was to determine which particular parameter to vary. Previous studies focused mainly on adjusting the activation energy (Chitsomboom and Northam, 1991; Segal and Haj-Hariri, 1994) and pre-exponential terms (Winowich, 1990). Aly (1991) varied each of these parameters for a generic Arrhenius equation, and studied the effect upon the reaction rate. It is important to note that aside from ignition, a steady state physical characteristic needs to be addressed, namely the distribution of the reaction zone. Reaction models are calibrated to provide an accurate comparison to experimentally measured flame thickness. The flame thickness measured however, is usually based on an opposed jet flame experiment for which the flame is a thin sheet rather than the distributed shape present in a combustor or afterburner. Aly found that modifying either the pre-exponential factor or activation energy spreads the reaction zone as they are decreased and increased respectively. This demonstrated that modifying either of these parameters would produce the desired stretching of the flame as well as compensating for the ignition effects. Thus, the choice was narrowed down to two parameters: activation energy and the pre-exponential factor. Ultimately, a parabolic dependence of the activation energy on temperature was selected, primarily because the reaction rate is more sensitive to changes in activation energy than changes in the pre-exponential factor. The parabolic relationship was clipped to a constant value below a critical low temperature limit and above a high temperature limit (500 K and 2500 K in these studies).

Numerical Approach. Numerical integration of the governing equations is achieved using an explicit, first-order, finite-difference approximation to the flux-split characteristic form of the hyperbolic partial differential equations (Kneile and Hale, 1995). The finite-difference equation for this scheme is:

$$\left(\frac{\Delta\bar{U}}{\Delta t}\right)_j = I^+_{j-\frac{1}{2}}\left[\bar{G}_{j-\frac{1}{2}} - \frac{\left(\bar{F}_j - \bar{F}_{j-1}\right)}{\left(x_j - x_{j-1}\right)}\right] + I^-_{j+\frac{1}{2}}\left[\bar{G}_{j+\frac{1}{2}} - \frac{\left(\bar{F}_{j+1} - \bar{F}_j\right)}{\left(x_{j+1} - x_j\right)}\right] \qquad (8)$$

where first-order Euler integration is used to advance the solution in time. In this equation, the I matrices pre-multiplying the square bracketed terms on the right hand side involve the eigenvalues of the Jacobian matrix and the + and – superscripts indicate right-running

and left-running characteristics, respectively. Notice that the fluxes are evaluated at the grid points whereas the / matrices and the source term vector are evaluated at the cell interfaces. In order to evaluate these quantities at the cell interface, variables are approximated by an Roe averages (Hirsch, 1990). A stable time step for the scheme is chosen as the more restrictive of a CFL based time step and a chemistry based time step (Drummond, et al., 1996). More details and a derivation of the method are given by Costura (1997).

Boundary Conditions. Characteristic-based boundary conditions, extended for reacting flow, are enforced at the inlet and exit of the computational domain (Kneile and Hale, 1995). At the inlet, total temperature, total pressure and species mass fractions are specified. At the outlet, either static pressure, mass flow rate, or Mach number are specified. Characteristic equations corresponding to the outgoing characteristics at the exit, *i.e.* the u and u+a (where a is the sound speed), and outgoing characteristics at the inlet, *i.e.* the u-a, are computed based on a subsonic boundary assumption. The boundary conditions are developed in order to be fully functional with a full engine simulation, including events such as engine surge. For this purpose, during reverse flow the inlet boundary condition is transitioned to a static pressure boundary condition. Upon resumption of forward flow, the upstream stagnation boundary conditions are increased at a user specified rate until the values match those specified before the reverse-flow event was encountered (Garrard, 1995). Essentially, this is similar to a compressor recovery in the full engine simulation.

RESULTS AND DISCUSSION

The combustor liner geometry to be evaluated is shown in Figure 1. This is a simple, swirl and cross jet stabilized can-type combustor that is undergoing testing as part of this research effort. The experimentally determined flow splits for this combustor are presented in Table 1, and further details on the geometry and experimental data are given by Costura (1997). The combustor is liquid fueled. In the experimental studies, the combustor was fired with ethyl alcohol, due to the need for a high volatility fuel to minimize the effects of spray quality. This introduces some error due to the large latent heat of vaporization, however, which is not currently modeled in the code.

Steady State Simulation

Numerical predictions for the experimental combustor geometry under non-reacting (cold) flow conditions are first examined. For this test case, the inlet total temperature, pressure and mass flow rate are 311 K, 275.6 kPa, and 0.272 kg/s, respectively. Injection of gaseous ethyl alcohol occurs just upstream of the primary zone at a rate of 22.7 L/hr to coincide with the experimental testing. Figure 2 shows the geometry, computational grid and boundary conditions, where 161 uniformly spaced grid points are employed in the simulations. The S and I indicators correspond to the swirler and fuel injector locations. The numbers indicate liner holes. The percentage of air which passes through the swirler slots and the primary, intermediate and dilution liner holes is measured in the laboratory and specified in the code. Losses associated with the swirlers are not accounted for in this preliminary test and the slot air injection is specified with zero streamwise momentum. Constant inlet total temperature, pressure and exit static pressure are enforced. Steady-state is achieved after 0.25 s. Figure 3 shows the steady-state velocity distribution within the combustor. The velocity decreases as the flow enters the diffuser and again when the flow is split before it enters the swirlers and the primary zone. The velocity increases as fuel is injected and as air is reintroduced into the combustor through the liner holes. The velocity increases further as the flow enters the exhaust section and exits the combustor at a slightly higher velocity than when it entered due to the additional fuel mass.

Simulations of steady state reacting flow are next examined. Initial conditions for this test case were identical to the cold flow study with the exception of the dilution air splits. In this test case, the three rows of the primary zone, and the three rows of the secondary zone were lumped into one injection port for each group with the amount of dilution air in each zone remaining the same as the cold flow case.

At the beginning of the simulation fuel begins to be injected at a constant equivalence ratio of 1.81 which approximates the primary zone equivalence ratio calculated in the laboratory tests, and the ignitor is activated to elevate the ignitor control volume by 200 K. Figure 4 shows temperature profiles at 0.30 and 0.60 seconds for the portion of the computational domain between x/L=0.4 and x/L=0.8. Until the ignitor source term is deactivated at 0.30 seconds, the solution reaches a steady state following the ignition event. When the ignitor source term is removed, the primary zone temperature decreases by 200 K as the flow reaches a second steady solution indicated by the profile given at 0.60 seconds. The predicted exit temperature is in good agreement with the experiments, with an exit temperature between 650 K and 700 K observed in the data.

Figure 5 presents a trace of the total temperature at x/L=0.56 which is located just downstream of the primary zone. Once again the effect of turning off the ignitor is seen at 0.30 seconds, with the temperature profile dropping nearly 100 K before becoming stable at approximately 1300 K. Since the primary zone dilution air has been added, only 50 K of the temperature drop can be attributed to the ignitor. The remainder of the temperature drop is due to a slight shift in the temperature profile where the reaction zone has elongated due to the absence of the preheat provided by the ignitor source term. In other words, at this location the fuel is no longer completely burned as it was in the previous steady state solution presented at 0.30 s.

Lean Blow Out Simulation

Results from a lean blow out simulation are achieved with initial conditions identical to the previous test case with the ignitor source term turned off at 0.30 seconds. At 0.40 seconds, the fuel injector mass flow rate is reduced to decrease the equivalence ratio at a rate of 1.0 per second. A plot of the exit total temperature trace is given in Figure 6. Over the period from 0.40 to 1.30 seconds, there is a gradual decline in exit temperature as the fuel flow rate is decreased. After a brief transient event at approximately 1.35 seconds, lean blowout is achieved at a primary zone equivalence ratio of 0.8, as indicated by the sharp decline in exit temperature. The exit fuel mass fraction trace also provided in Figure 6 indicates the presence of unburned fuel as a result of the injector remaining active until the end of the simulation.

Upon achieving lean blowout, a large disturbance is evident in the mass flow rate which is presented in Figure 7. Following the spike, a self-sustaining oscillation is evident with an approximate frequency of 100 Hz. This may be explained by a brief reverse flow event which occurs just upstream of the combustion liner where the secondary air is extracted. This event causes the secondary air

source term to shut off. due to the current numerical formulation of the source term, until the flow recovers. The subsequent occurrence of reverse flow oscillations induced at this axial location corresponds to the exact frequency of the exit mass flow rate oscillations, which would suggest that the source term is driving the flow into this perpetual instability.

An experimental test of lean blowout in this combustor has been perfomed (Costura, 1997) with an equivalence ratio change identical to the above simulation. In Figure 8, data from high response thermocouples located in the primary zone of the combustor and the exit plane are shown. Here the primary zone temperatures are used primarily as an indication of flame position, as radiation effects are significant and reduce temperature accuracy. However, it is clear that primary zone temperatures are similar to those predicted previously in Figure 4. Of significance in the lean blow out transient is the change in character of the primary zone trace at t=13.4 s, followed by a sharp decay in primary zone temperature. This occurs at an exit temperature of 450 K, and is consistent with termination of flame in the primary zone. This exit temperature value compares favorably to the 500 K value indicated by the simulation at lean blowout.

CONCLUSIONS

A combustor model was developed to study gas turbine dynamics. The model was tested for both cold and hot flow in can-type gas turbine combustor geometry. Comparisons to the available experimental data were favorable. Results from the combustor model and transient combustor test data show that:

(1) Cold flow simulations performed with the test combustor geometry demonstrated the models ability to provide a stable solution while diverting large quantities of mass flow required to model the effect of flow splitting.

(2) In addition to the detection of unburned fuel and decreasing exit temperature, lean blowout simulations showed similarities to the behavior exhibited in the experimental data.

In addition, the current studies have illuminated the need for a revision of the current secondary mass flow model, as this proved inadequate to provide accurate results for large scale flow disturbances such as that resulting from lean blowout. In addition, although adequate for a first approximation, the assumptions of infinite mass transfer rate between the extraction and injection ports and fixed flow split information in this model need to be re-evaluated in the future. In order to alleviate these concerns, it should be possible to parallel process the secondary air passage using the extraction node as the inlet boundary and the final injection port as the exit boundary. The intermediate injection holes would then be calculated as bleed terms based upon the pressure differential across the liner interface.

As a broader range of data from the experimental program becomes available, it is foreseen to continue to exercise and develop this model against that database, with a focus on rich blow out and reverse flow events.

ACKNOWLEDGMENTS

This work was supported by the Arnold Engineering Development Center under the Joint Dynamics Air-Breathing Propulsion Simulation (JDAPS) working group. The authors would like to thank Dr. Milt W. Davis and Dr. Doug Garrard of Sverdrup Technology, Inc. AEDC Group, for their assistance with this project.

REFERENCES

Aly, S.L., "Flame Structure and Reaction Kinetics: The Effects of the Pre-exponential Frequency Factor, Reaction Order, and Activation Energy", *Applied Energy*, Vol. 37, pp. 139-150, 1991.

Ayoub, N.S., and R.D. Reitz, "Multidimensional Modeling of Fuel Effects and Split Injections on Diesel Engine Cold-Starting", *Journal of Propulsion and Power*, Vol. 13, No. 1, Jan.-Feb. 1997.

Chitsomboon, T., and G.B. Northam, "Computational Fluid Dynamics Prediction of the Reacting Flowfield Inside a Subscale Scramjet Combustor", *Journal of Propulsion*, Vol. 7, No. 1, Feb. 1991.

Costura, D.M., "A Computaional and Experimental Study of Gas Turbine Combustor Dynamics." M.S. Thesis, Purdue University, West Lafayette, Indiana, December 1997.

Costura, D.M., Velez, T.A., Lawless, P.B., and S.H. Frankel, "A Model for Combustor Dynamics for Inclusion in a Dynamic Gas Turbine Engine Simulation Code," AIAA-97-3336, 1996.

Davis, M.W., "A Statge-by-Stage Post-Stall Compression System Modeling Technique: Methodology, Validation, and Application", PhD Dissertation, Virginia Polytechnic Institute and State University, 1986.

Drummond, J.P., Rogers, R.C., and M.Y. Hussaini, "A Detailed Numerical Model of a Supersonic Reacting Mixing Layer." AIAA-86-1427, 1996.

Egolfopoulos, F.N., Du, D.X., and C.K. Law, "A Study on Ethanol Oxidation Kinetics in Laminar Premixed Flames, Flow Reactors, and Shock Tubes", Twenty-Fourth Symposium (International) on Combustion, The Combustion Institute, pp. 833-841, 1992.

Garrard, G.D., Davis, M.W. Jr., and A.A. Hale, "Recent Advances in Gas Turbine Engine Dynamic Models Developed Through JDAPS." ASME Paper 95-GT-146, 1995.

Garrard, G.D., "ATEC: The Aerodynamic Turbine Engine Code for the Analysis of Transient and Dynamic Turbine Engine System Operations," Ph.D. Dissertation, The University of Tennessee, Knoxville, August, 1995.

Hale, A.A., and M.W. Davis, "Dynamic Turbine Engine Compressor Code DYNTECC - Theory and Capabilities," AIAA Paper 92-3190, 1992.

Hirsch, C., *Numerical Computation of Internal and External Flows*, John Wiley & Sons, New York, 1990

Kong, S.C., and R.D. Reitz, "Multidimensional Modeling of Diesel Ignition and Combustion using a Multistep Kinetics Model".

Journal of Engineering for Gas Turbines and Power, Vol. 115, pp. 781-789, Oct. 1993.

Kneile, K.R., and A.A. Hale, "Appendix C: Numerical Solution to the Governing Equations," Appendix C in Garrard, Ph.D. Dissertation, The University of Tennessee, Knoxville, August, 1995.

Lefebvre, A.H., *Gas Turbine Combustion*, Taylor & Francis, 1983

Mellor, A.M., "Gas Turbine Engine Pollution", *Prog. Energy Combust. Sci.* 1, 111-133, 1976

Przybylko, S.J., "Application of System Identification Techniques to Poststall Combustor Dynamics." AIAA Paper 85-1353, 1985.

Segal, C., and H. Haj-Hariri, "Effects of the Chemical Reaction Model on Calculations of Supersonic Combustion Flows", *Journal of Propulsion*, Vol.11, No. 3. 1994.

Vlachos, D.G., "Reduction of Detailed Kinetic Mechanisms for Ignition and Extinction of Premixed Hydrogen/Air Flames", *Chemical Engineering Science*, Vol. 51, No.16, pp. 3979-3993, 1996.

Westbrook, C.K., and F.L. Dryer, "Simplified Reaction Mechanisms for the Oxidation of Hydrocarbon Fuels in Flames," *Combustion Science and Technology*, Vol. 27, pp. 31-43, 1981.

Winowich, N.S., "Numerical Prediction of Turbulent Flame Stability in Premixed/Prevaporized (HSCT) Combustors," National Aeronautics and Space Administration Contractor Report NASA-CR-188991, 1990.

Table 1. Flow Splitting Information at Test Operating Point

Physical Location	%
Inlet Swirl Slots	8.0
1st Primary Row	16.0
2nd Primary Row	23.5
3rd Primary Row	31.0
1st Secondary Row	40.3
2nd Secondary Row	49.6
3rd Secondary Row	59.0
Dilution/Annulus	100.0

Figure 1. Photograph of Combustor Liner.

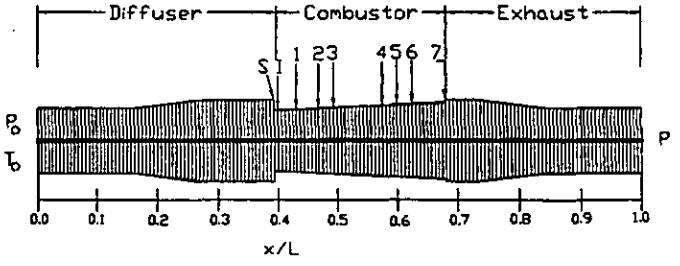

Figure 2. Computational Grid, Physical Diagram and Boundary Conditions for Test Combustor Geometry.

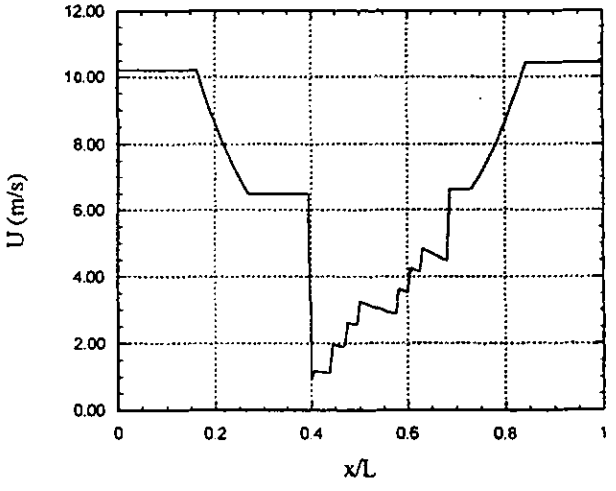

Figure 3. Steady State Velocity Profile for Cold Flow Test

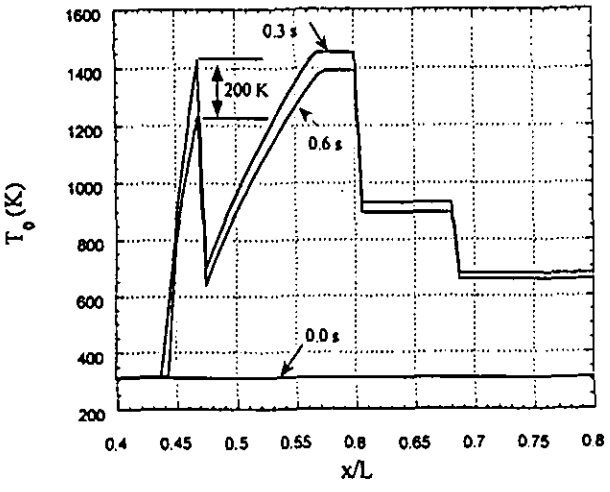

Figure 4. Total Temperature Profiles for Steady Reacting Flow

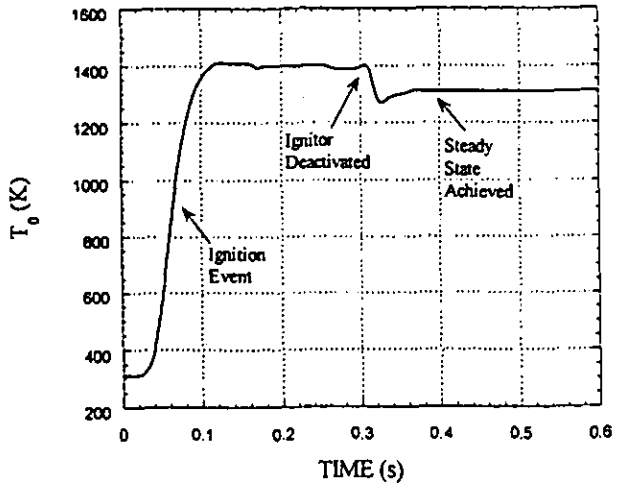

Figure 5. Total Temperature Trace at x/L = 0.56 for Steady Reacting Flow Test Case.

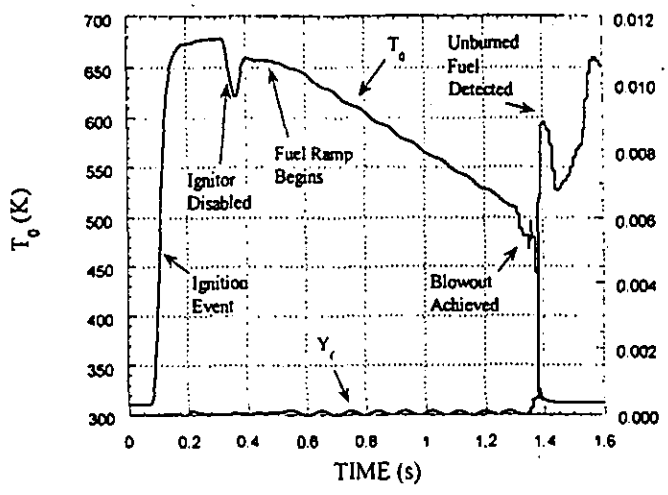

Figure 6. Exit Total Temperature Trace and Fuel Mass Fraction Trace for the Lean Blowout Transient Test Case.

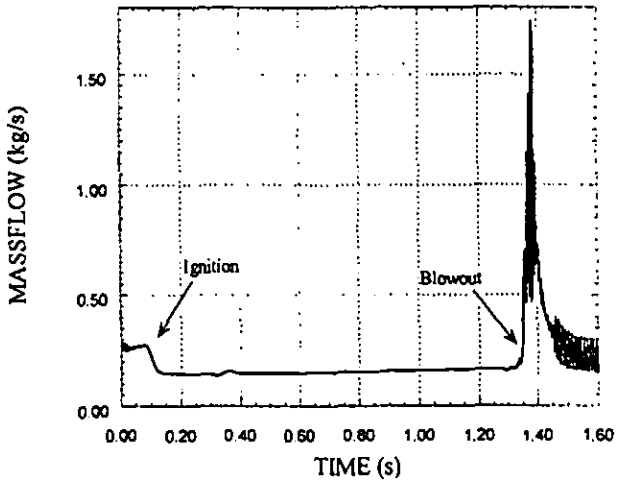

Figure 7. Exit Mass Flow Rate Trace for Lean Blowout Transient

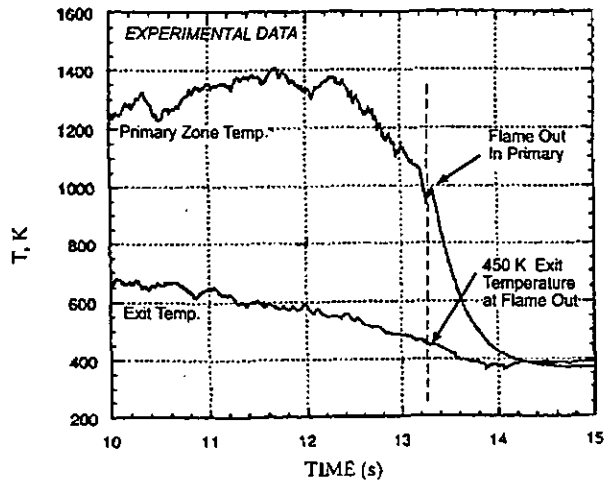

Figure 8. Exit Total Temperature and Primary Zone Temperature for the Lean Blowout Testing over the Period t = 10.0 s until t = 15.0 s.